Research Square

Preprints are preliminary reports that have not undergone peer review.
They should not be considered conclusive, used to inform clinical practice,
or referenced by the media as validated information.

Enhancing plant establishment via rhizosphere signaling and hormonal regulation through biopolymer-mediated soil pore restructuring

Kaniz Fatema

kaniz.fatema@stonybrook.edu

Stony Brook University https://orcid.org/0000-0002-1615-5918

Aaron Sloutski
Yiwei Fang
Xiaoyang Liu
Jay G. Gao
Marcia Simon
Eyal Zussman
Vitaly Citovsky
Miriam Rafailovich
https://orcid.org/0000-0002-9483-5812

Research Article

Keywords: Rhizosphere, plant establishment, root development, microbial biopolymers, soil microstructure, plant-soil interactions

Posted Date: June 8th, 2026

DOI: https://doi.org/10.21203/rs.3.rs-9829620/v1

License: This work is licensed under a Creative Commons Attribution 4.0 International License.
Read Full License

Enhancing plant establishment via rhizosphere signaling and hormonal regulation through biopolymer-mediated soil pore restructuring

Kaniz Fatema[1], Aaron Sloutski[1, *], Yiwei Fang[1], Xiaoyang Liu[2], Jay G. Gao[3], Marcia Simon[3], Eyal Zussman[4], Vitaly Citovsky[5], Miriam Rafailovich[1, *]

[1]Department of Materials Science and Chemical Engineering, State University of New York at Stony Brook, Stony Brook, New York 11794, USA.

[2]Advanced Photon Source, Argonne National Laboratory, Lemont, Illinois 60439, USA.

[3]Department of Oral Biology and Pathology, School of Dental Medicine, Stony Brook University, Stony Brook, NY, 11794, USA.

[4]Faculty of Mechanical Engineering, Technion-Israel Institute of Technology, Haifa.

[5]Department of Biochemistry and Cell Biology, State University of New York at Stony Brook, Stony Brook, New York 11794, USA.

[*]Corresponding author (Email: miriam.rafailovich@stonybrook.edu).

Keywords

Rhizosphere; plant establishment; root development; microbial biopolymers; soil microstructure; plant-soil interactions

Abstract

Aims

Coarse-textured sandy soils impose major constraints on plant establishment due to low cohesion, rapid drainage, and limited regulation of rhizosphere water and nutrient availability. We evaluated ethanol-precipitable material (EPM), a microbially derived extracellular biopolymer from Rhizobium tropici, as a soil amendment and compared its effects with xanthan gum (XG) to determine how biopolymer-mediated pore restructuring influences root development and plant performance.

Methods

Synchrotron X-ray micro-computed tomography (μCT) and unconfined compressive strength testing were used to characterize changes in soil pore architecture and mechanical behavior. Plant growth responses were quantified through biomass and root morphology measurements. Elemental composition was determined by X-ray fluorescence (XRF), while RNA sequencing (RNA-seq) and RT-qPCR were used to assess transcriptional responses associated with root development.

Results

Both biopolymers increased soil strength and reduced porosity; however, they generated distinct pore architectures. EPM produced spatially uniform reinforcement while maintaining pore connectivity, whereas XG induced localized densification and increased pore heterogeneity. EPM significantly enhanced plant establishment, increasing Bermuda grass biomass by more than fourfold and promoting extensive root proliferation, while XG provided little or no growth benefit. Elemental analysis indicated improved nutrient acquisition under optimal EPM concentrations. Transcriptomic and RT-qPCR analyses revealed coordinated regulation of cytokinin turnover, auxin-associated signaling, flavonoid biosynthesis, and redox pathways, consistent with enhanced lateral root development.

Conclusions

EPM-mediated pore restructuring promotes plant establishment by maintaining rhizosphere accessibility while enhancing soil stability. These findings identify pore architecture as a key regulator linking root developmental responses and plant performance in degraded sandy soils.

Abbreviations

EPM = Ethanol precipitable material, EPS = Extracellular polymeric substances, XG = Xanthan gum, μCT = micro-computed tomography, UCS = unconfined compressive strength, APS = Advanced photon source, ANOVA = Analysis of variance, Tukey's HSD = Tukey's Honestly Significant Difference, PCA = Principal component analysis, RT-qPCR = Reverse transcription-quantitative polymerase chain reaction, RNA-Seq = RNA sequencing, ROS = reactive oxygen species.

Introduction

Soil physical degradation, characterized by the loss of soil structure and redistribution of fine particles under rainfall, wind, and anthropogenic disturbance, remains one of the most critical drivers of global land degradation (Lal 2001). This process results in the preferential loss of nutrient-rich topsoil, leading to reduced soil fertility, diminished water retention, and long-term declines in ecosystem functioning. Although part of natural geomorphic and pedological processes, these structural alterations are significantly intensified by vegetation loss, intensive agriculture, and land-use change associated with urbanization and infrastructure development. With nearly one-third of global soils already degraded, developing effective and environmentally sustainable strategies for soil structural stabilization and restoration is an urgent priority.

Biopolymer-based amendments have emerged as promising environmentally compatible approaches for mitigating soil erosion by improving interparticle bonding and increasing soil strength at low application rates (Raj et al. 2023). These materials are attractive because they are derived from natural or bio-based sources and can temporarily enhance soil structural stability without introducing persistent synthetic contaminants. However, their effectiveness is often limited in natural environments, where rainfall infiltration, wetting-drying cycles, and microbial activity can lead to polymer dissolution, leaching, or degradation, resulting in a gradual loss of reinforcement. Indeed, optimal performance has been reported within relatively short curing periods (e.g., ~28 days for biopolymer-treated clays) (Cheng and Geng 2023), highlighting the transient nature of their mechanical benefits.

This limitation underscores the need to move beyond short-term physicochemical stabilization toward more persistent soil functional recovery strategies. One promising direction is to couple initial soil stabilization with biological reinforcement processes that support vegetation establishment and long-term root-mediated soil cohesion. In this context, soil structure plays a central role, as it regulates both mechanical resistance to root penetration and the transport of water, gases, and nutrients within the soil matrix (Kolb et al. 2017). This is particularly critical in coarse-textured sandy soils, where low cohesion and limited fine particles result in weak structural stability and poor water retention (Osman 2018).

While biopolymers can improve soil strength, they also alter pore-scale architecture. Excessive pore constriction may increase mechanical impedance, reduce gas diffusion, and restrict root growth (Bengough et al. 2006), whereas pore-permissive modifications can simultaneously support soil stability and biological activity. Therefore, achieving an optimal balance between soil reinforcement and pore accessibility represents a key unresolved challenge in designing environmentally sustainable soil amendment strategies.

Importantly, changes in soil physical structure act not only as mechanical modifications but also as biologically relevant signals. Roots perceive mechanical impedance, hydration status, and oxygen availability, integrating these cues through coordinated hormonal and stress-response pathways, including auxin-cytokinin crosstalk and redox regulation. These signaling networks regulate root system architecture, particularly lateral root initiation and spatial proliferation, thereby linking soil physical conditions to plant developmental outcomes. However, the extent to which biopolymer-induced alterations in soil structure interact with these molecular regulatory pathways remains poorly understood.

Extracellular polymeric substances (EPS) produced by soil microorganisms represent a class of naturally derived biopolymers capable of simultaneously influencing soil structural properties and plant responses (Palhares Farias et al. 2022), (Feng et al. 2026). In particular, ethanol-precipitable material (EPM) derived from *Rhizobium tropici* has been reported to enhance soil stability and promote plant growth at low application rates (~0.01–0.5 wt%) (Nestler et al. 2016), (Sloutski et al. 2025), in addition to improving soil aggregation and water retention characteristics (Larson et al. 2012). More recent work has focused on isolating mechanistically active fractions of this material, where ethanol-precipitable EPM exhibits pronounced gel-forming behavior and modifies particle-water interactions at the pore scale (Yiwei Fang et al. 2025). Despite these advances, the mechanistic links between EPM-induced physical changes in soil structure and downstream regulation of plant developmental processes remain unresolved.

In this study, we investigate how EPM-mediated modifications of soil mechanical properties and pore architecture influence root development and overall plant performance in both model sandy systems and agronomically relevant soils. We integrate mechanical testing and three-dimensional pore-network characterization with plant phenotyping and transcriptomic analysis to capture coupled soil-plant responses across scales. We hypothesize that environmentally stable and erosion-resistant soil systems emerge not from maximal mechanical strengthening, but from a balance between structural stability and pore accessibility that supports root establishment and activates adaptive developmental programs underlying sustained soil function.

Materials and Methods

EPM was isolated from *Rhizobium tropici* culture supernatants by ethanol precipitation and reconstituted in water to generate stock solutions for soil amendment and plant assays. To evaluate the mechanical effects of EPM on granular substrates, sand was amended with defined concentrations of EPM or xanthan gum (XG) as a reference biopolymer. XG was selected because it is among the most effective and widely studied biopolymers for soil stabilization, consistently reported to yield comparatively high strength and stiffness relative to other candidates such as chitosan, guar gum, alginate, and glucan, owing to its viscous gel formation and particle-bridging behavior (Soldo et al. 2020). Cylindrical specimens were prepared under standardized mixing and compaction conditions, cured under controlled environmental conditions, and subjected to unconfined compressive strength (UCS) testing to quantify stress-strain behavior and peak strength.

The micro-CT experiment was conducted at the 7-BM beamline, Advanced Photon Source (APS) of Argonne National Laboratory. The white beam was filtered with 350 μm Cu foil. The detector-to-sample distance is 300 mm to enhance the phase contrast of sand. For the imaging system, 10× objective lens was used to result in effective image pixel size of 0.69 μm. For the tomographic scan, 2561 projections were collected over a 180-degree rotation with exposure time of 0.12 s per frame. TomocuPy (Nikitin 2023) package was used for image reconstruction.

Porosity was quantified from a cubic region of interest (~1.57 × 1.57 × 1.67 mm^3), corresponding to 2268 × 2268 pixels in-plane and 2426 slices axially. Image processing and segmentation were performed in Fiji (ImageJ), and porosity was calculated using the BoneJ plugin based on the ratio of void volume to total volume.

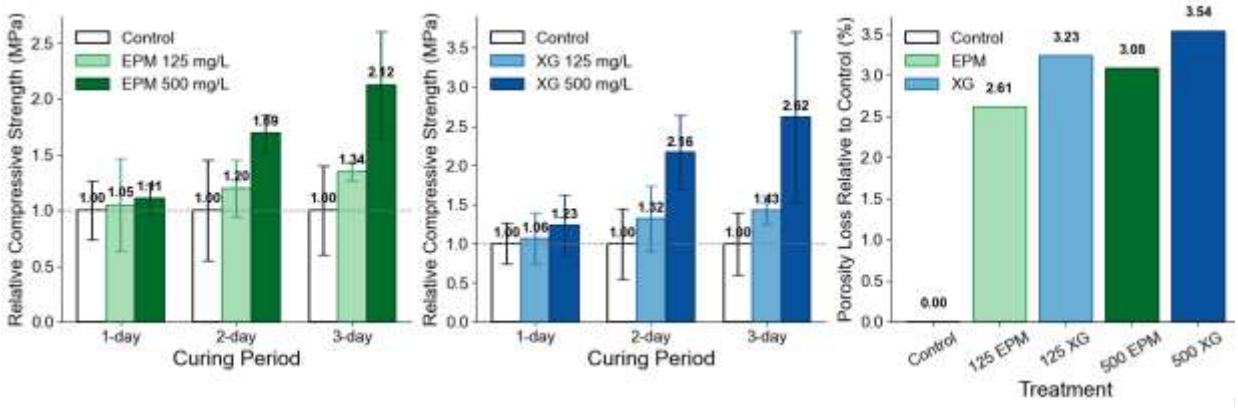
Plant growth responses were assessed in *Cynodont dactylon* (Bermuda grass), *Phaseolus vulgaris* (bush bean), and *Arabidopsis thaliana* (Thale cress) grown in EPM-amended sand or soil under controlled greenhouse conditions. Biomass allocation in plant, morphology of root, and fruit production was quantified at harvest. For molecular analyses, root tissue was collected, RNA was extracted, reverse-transcribed to cDNA, and gene expression was quantified by qPCR. Detailed experimental procedures are provided in the **Supplementary data file (Fig. S1, S2, S3, and S4)**.

Results

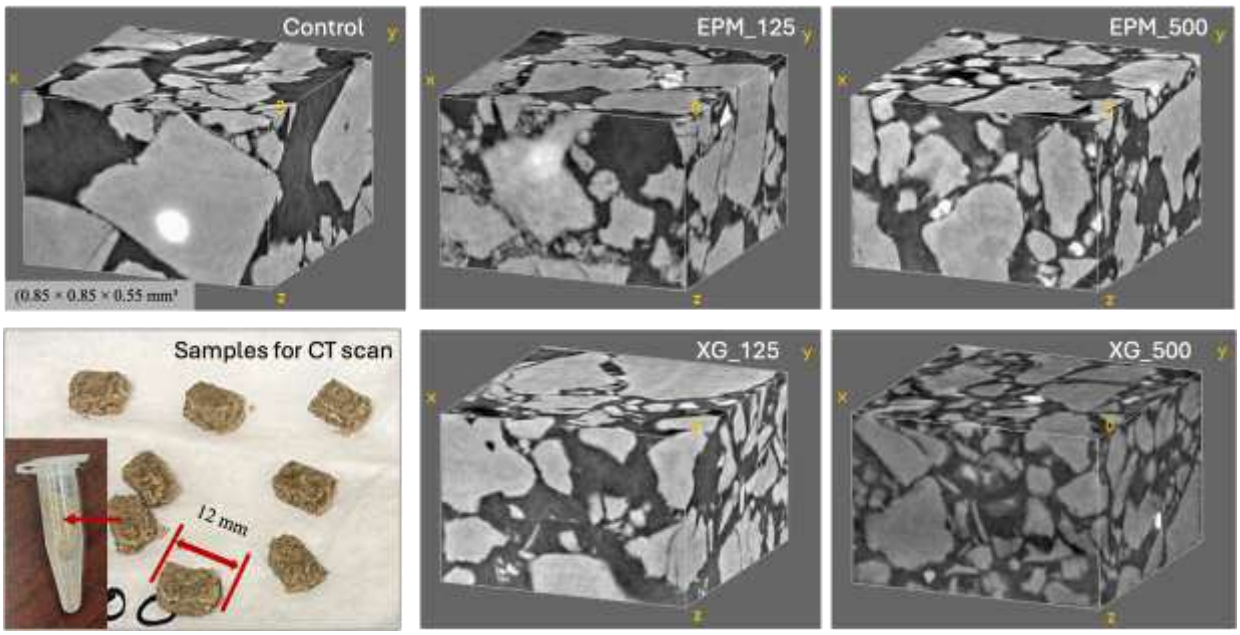
Biopolymer-mediated modification of soil structure

Washed play sand was used as a model coarse-textured system to isolate the effects of biopolymer amendment on soil structural behavior and plant-relevant properties. Untreated sand exhibited nearly constant unconfined compressive strength (UCS) across curing times (**Supplementary Fig. S5**), indicating negligible intrinsic cohesion. Specimens were cured for up to 3 days to capture the pre-irrigation strengthening phase relevant to plant growth conditions.

Biopolymer amendment resulted in distinct, chemistry-dependent changes in soil structural stability. Ethanol-precipitable material (EPM) produced a moderate, concentration-dependent increase in strength (≈1.05-2.12) with relatively low variability, whereas xanthan gum (XG) generated larger and more curing-sensitive increases (up to ≈2.62), particularly at higher concentrations (**Figure 1a**). Changes in porosity further supported these distinctions. At 125 mg L^{-1}, porosity reduction was modest for EPM (2.61%) and slightly higher for XG (3.23%), while at 500 mg L^{-1} both polymers produced slightly greater reductions. Micro-computed X-ray tomography (μCT) revealed that these bulk changes corresponded to distinct pore-scale architectures (**Figure 1b**). EPM-treated systems maintained relatively homogeneous and well-connected pore networks, whereas XG promoted aggregation of finer particles into consolidated regions adjacent to larger voids, resulting in heterogeneous pore distribution and increased tortuosity.



(a)



(b)

Figure 1* | *Unconfined compressive strength and pore morphology.

(a) Relative compressive strength of EPM and XG-amended sand normalized to the untreated control.

Left panel: Compressive strength ratios (sample strength divided by control strength) for sand treated with EPM at 0 (control), 125, and 500 mg L^{-1} after 1, 2, and 3 days of curing (silt = 0%). Normalization highlights the modest, curing-dependent reinforcement provided by EPM, with controlled strength enhancement even at high concentration. Error bars represent relative standard deviation (sample standard deviation divided by control strength).

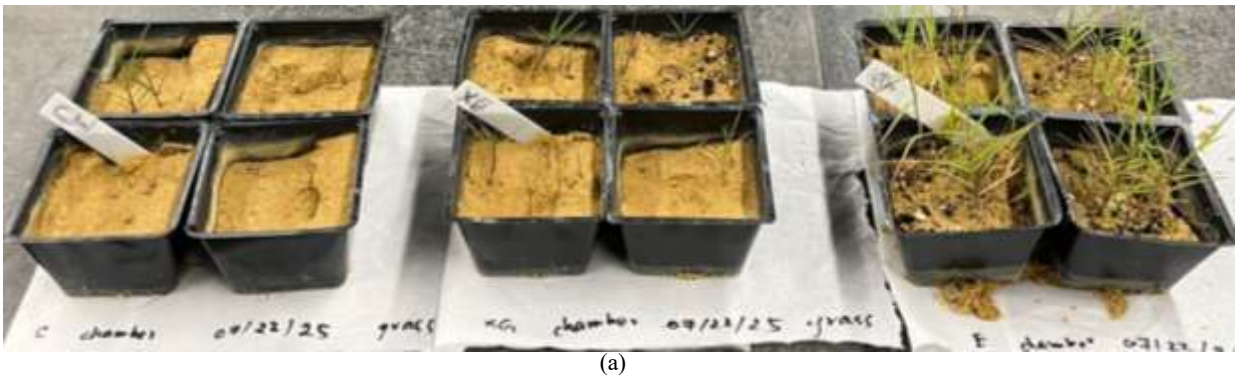
Middle panel: Compressive strength ratios for sand treated with XG at 0 (control), 125, and 500 mg L^{-1} after 1, 2, and 3 days of curing (silt = 0%). XG exhibits a pronounced concentration- and time-dependent increase in relative strength, particularly at 500 mg L^{-1}, consistent with strong particle bridging and matrix stiffening. Error bars represent relative standard deviation (sample standard deviation divided by control strength.

Right panel: Biopolymer-induced pore-scale restructuring in sand revealed by X-ray microtomography. Porosity loss relative to the untreated control, highlighting polymer- and concentration-dependent pore-space reduction.

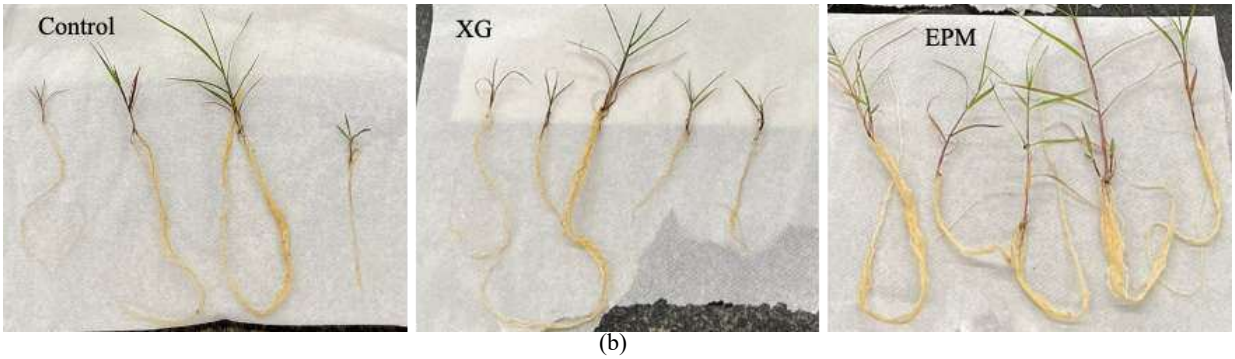
(b). Three-dimensional visualization of pore morphology along with samples for micro-CT. Volume renderings derived from micro-CT reconstructions for untreated sand and samples for tomography (column 1), EPM-amended sand (column 2), and xanthan gum–amended sand (column 3). EPM and XG concentrations of 125 and 500 mg L^{-1} are shown in the top and bottom rows, respectively. Volume views were generated from a region of interest measuring approximately 0.85 × 0.85 × 0.55 mm^3 (X × Y × Z; 1226 × 1226 pixels in-plane and 800 slices). Untreated sand exhibits a highly connected pore network, whereas biopolymer amendment results in progressive pore-space reduction, with XG producing denser and more heterogeneous structures compared with EPM.

Plant growth in sandy soils

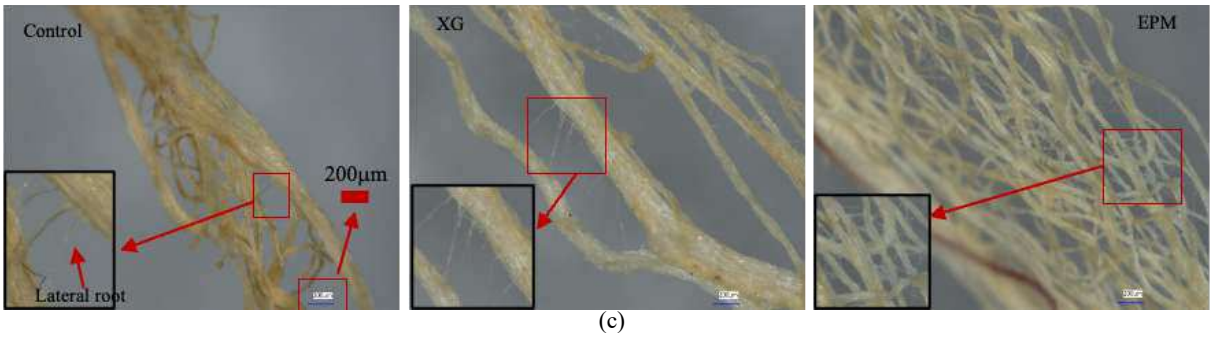
Given the distinct structural and pore-scale characteristics induced by EPM and XG, we evaluated how the modified soil environments influence plant establishment and root development. Bermuda grass (*Cynodon dactylon*) was grown in control, EPM-amended, and XG-amended sand at 125 mg L^{-1}, a concentration selected based on preliminary optimization. After six weeks, EPM-treated systems exhibited significantly greater shoot biomass and more extensive root systems compared to both control and XG treatments (**Figure 2 a-c**). Root morphology also differed among treatments. Plants grown in control and XG-amended sand developed relatively smooth roots with limited lateral branching. In contrast, EPM-treated plants displayed thicker roots and enhanced lateral root development, indicating greater root system complexity and increased soil exploration capacity.



(a)



(b)



(c)

Figure 2 | Visual validation of enhanced plant establishment in EPM-amended sand (125 mg L⁻¹).

(a) Bermuda grass grown in control sand, XG-amended sand, and EPM-amended sand under controlled chamber conditions.

(b) Plants harvested from control (left), XG-treated (middle), and EPM-treated (right) sand following washing and drying, showing enhanced shoot and root development in the EPM-treated samples.

(c) Roots from control (left), XG-treated (middle), and EPM-treated (right) plants. Roots from control and XG treatments exhibit relatively smooth morphologies with limited lateral root formation, whereas EPM-treated roots display increased thickness and a dense network of fine lateral roots, indicative of enhanced root development.

EPM amendment significantly enhanced plant growth, with substantial increases in total, root, and shoot biomass compared to the control (**Figure 3a-d**). Total biomass increased by more than fourfold ($p < 0.001$), driven primarily by pronounced root development, whereas XG treatment did not produce significant changes across any biomass metric. Shoot biomass increased proportionally with root biomass, and the shoot-to-root ratio remained consistent across treatments, indicating coordinated growth rather than major shifts in biomass allocation. For cross-trait comparison, biomass values were normalized to the control mean (**Supplementary Table S1**).

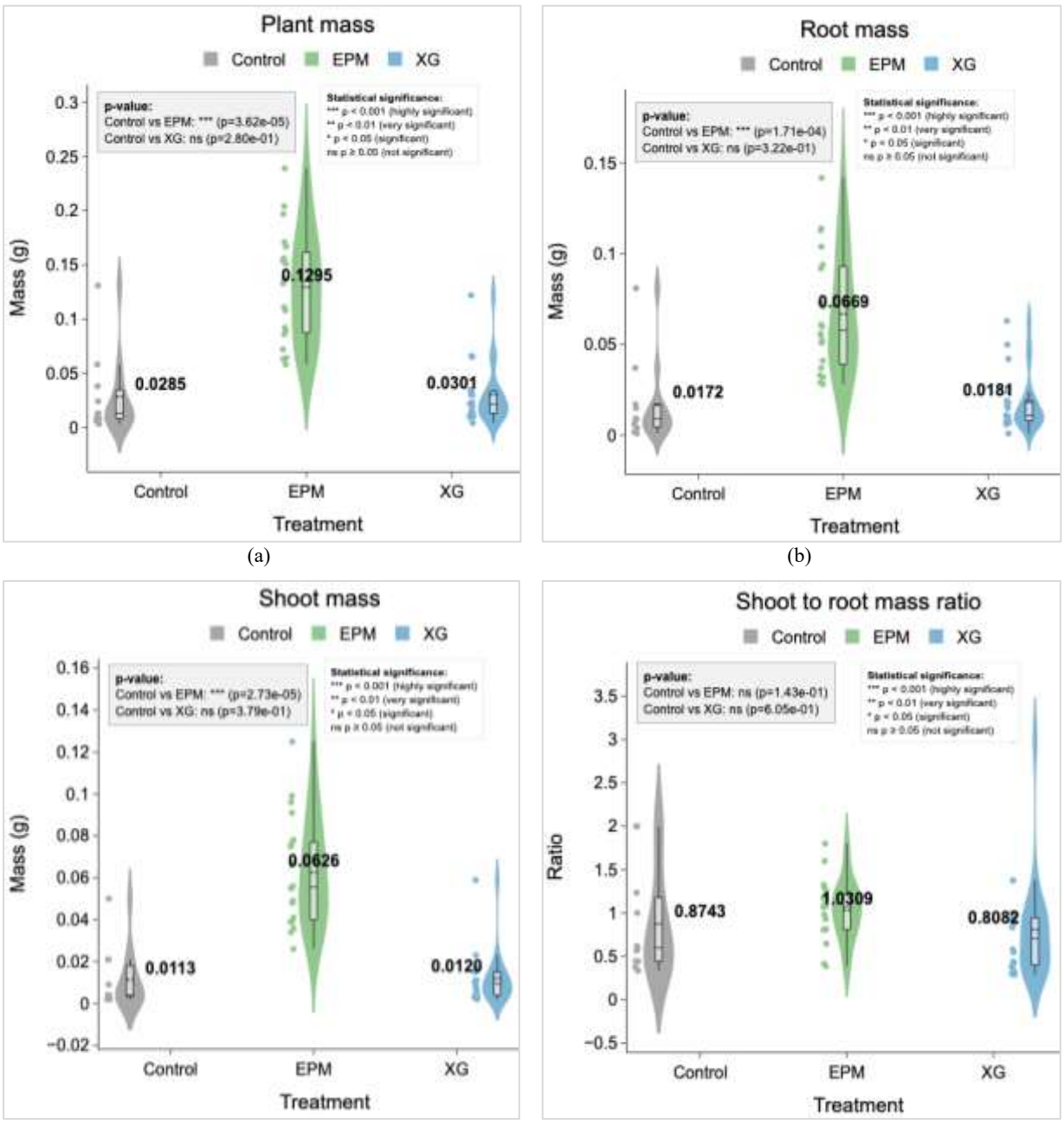


Figure 3 | Growth response of Bermuda grass in biopolymer-amended sand. *Violin plots showing the distribution of (a) total plant mass, (b) root mass, (c) shoot mass, and (d) shoot-to-root mass ratio for Bermuda grass grown in control sand, EPM-amended sand, and (XG)-amended sand. EPM-amended sand resulted in a pronounced increase in total biomass (average 0.1295 g) compared to both control (0.0285 g) and XG-treated sand (0.0301 g). Correspondingly, both root mass (0.0669 g) and shoot mass (0.0626 g) were significantly higher in the EPM system relative to the control ($p < 0.001$), whereas no statistically significant differences were observed between control and XG-treated sand across these metrics ($p > 0.05$). Despite the substantial increase in absolute biomass, the shoot-to-root mass ratio showed no significant variation among treatments, indicating proportional enhancement of above- and below-ground growth in the presence of EPM. Individual data points represent biological replicates; central boxes denote the interquartile range with median values, and statistical significance was assessed using two-sample t-tests with unequal sample sizes.*

Dose dependent plant response

EPM amendment induced a concentration-dependent response in bush bean (*Phaseolus vulgaris*) growth and root development (**Figure 4a-c**). Compared to the control, low to intermediate EPM concentrations (50 - 100 mg L^{-1}) enhanced root thickness, density, and lateral branching, indicating improved root system development and increased soil exploration capacity. At the highest concentration (500 mg L^{-1}), root systems exhibited the greatest biomass and structural complexity, forming dense and highly branched architectures. But surprisingly, despite this pronounced root proliferation, reproductive performance displayed a non-linear response. Pod production increased at 50 and 100 mg L^{-1}, with maximum yield observed at 100 mg L^{-1} but declined at 500 mg L^{-1} to levels below the control (**Figure 4c**). Elemental analysis of harvested pods (**Supplementary Fig. S6**) supported this trend, with macronutrient concentrations (Ca, K, and P) highest at the intermediate concentration.

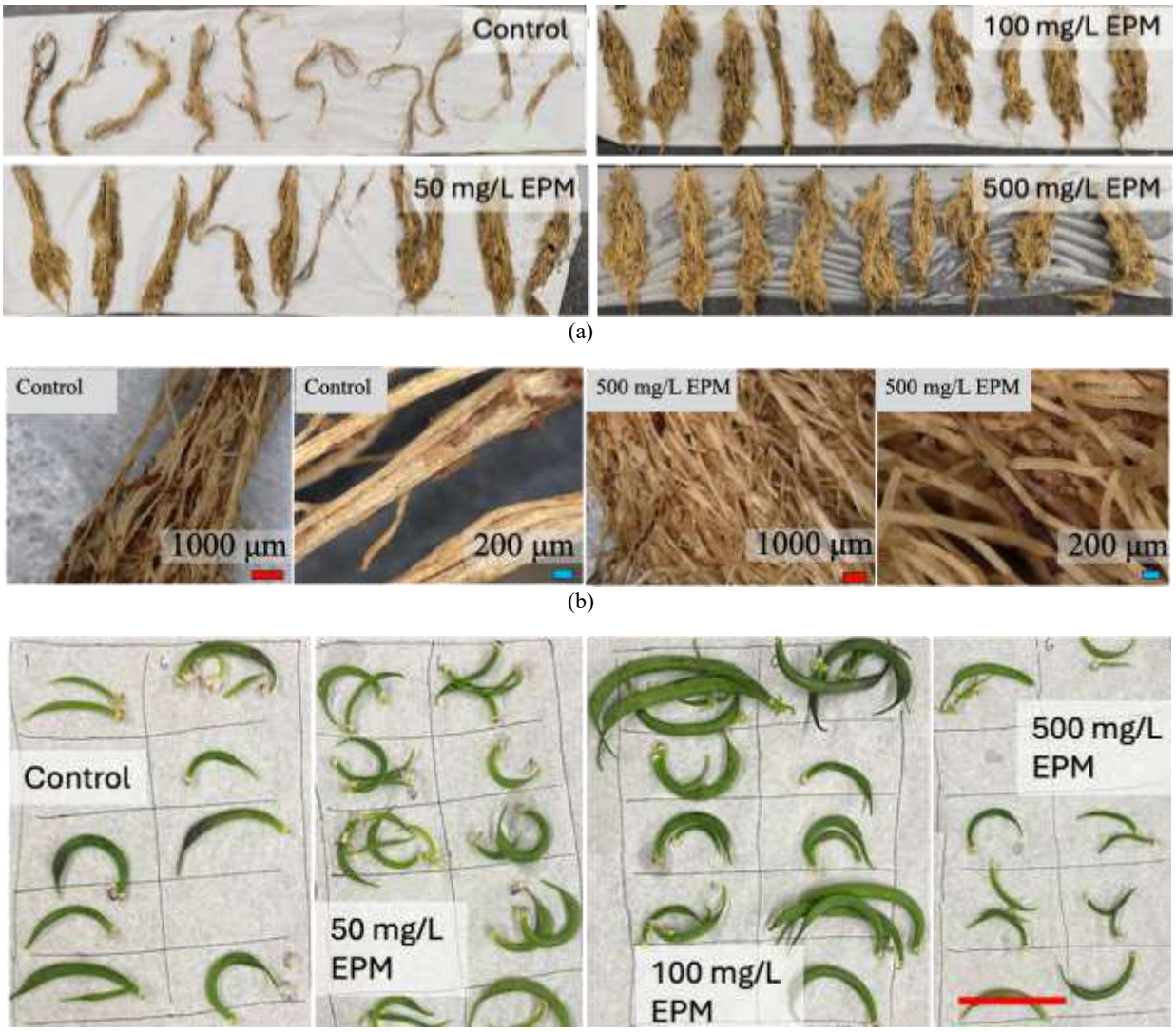


Figure 4 | Root morphology and bean pods of bush beans grown in garden soil amended with increasing concentrations of EPM.

(a) Control (0 mg L^{-1}EPM) roots are sparse, thin, and exhibit limited lateral expansion. At 50 mg L^{-1} EPM, roots display increased thickness, density, and fine-root proliferation relative to the control. Treatment with 100 mg L^{-1} EPM results in moderately

developed root systems, with improved branching compared to the control but less overall biomass than observed at 50 mg L⁻¹. At 500 mg L⁻¹ EPM, roots exhibit the most pronounced development, with substantially greater size, density, and architectural complexity, indicating enhanced below-ground biomass accumulation at the highest concentration tested.

(b) Microscopic analysis of roots. Bush bean roots were visualized following the removal of soil (scale bars: red = 1000 µm; blue = 200 µm). Control roots are thinner and less abundant. Roots from plants grown in soil amended with 500 mg L⁻¹ EPM are thicker and form a denser root network.

(c) Effects of EPM on bean pod formation. Representative images of bean pods harvested from individual plants grown in soil amended with different EPM concentrations, 0, 50, 100, and 500 mg L⁻¹ EPM. the highest production was observed at 100 mg L⁻¹ (scale bar = 10 cm).

EPM amendment significantly influenced bush bean growth and biomass allocation patterns (**Figure 5**). Total biomass increased with treatment (one-way ANOVA, $p < 0.001$), with Tukey's HSD indicating higher values at 50-500 mg L^{-1} compared to the control ($p < 0.05$). Root biomass exhibited a pronounced, dose-dependent response (ANOVA, $p < 0.001$), increasing significantly across all concentrations and reaching a maximum at 500 mg L^{-1}. In contrast, shoot biomass did not vary significantly among treatments (ANOVA, $p > 0.05$), indicating that increases in total biomass were primarily driven by enhanced belowground development. The shoot-to-root ratio varied significantly with treatment (ANOVA, $p < 0.001$), decreasing at intermediate concentrations and partially recovering at higher loading, reflecting a shift in biomass allocation toward root systems under EPM amendment.

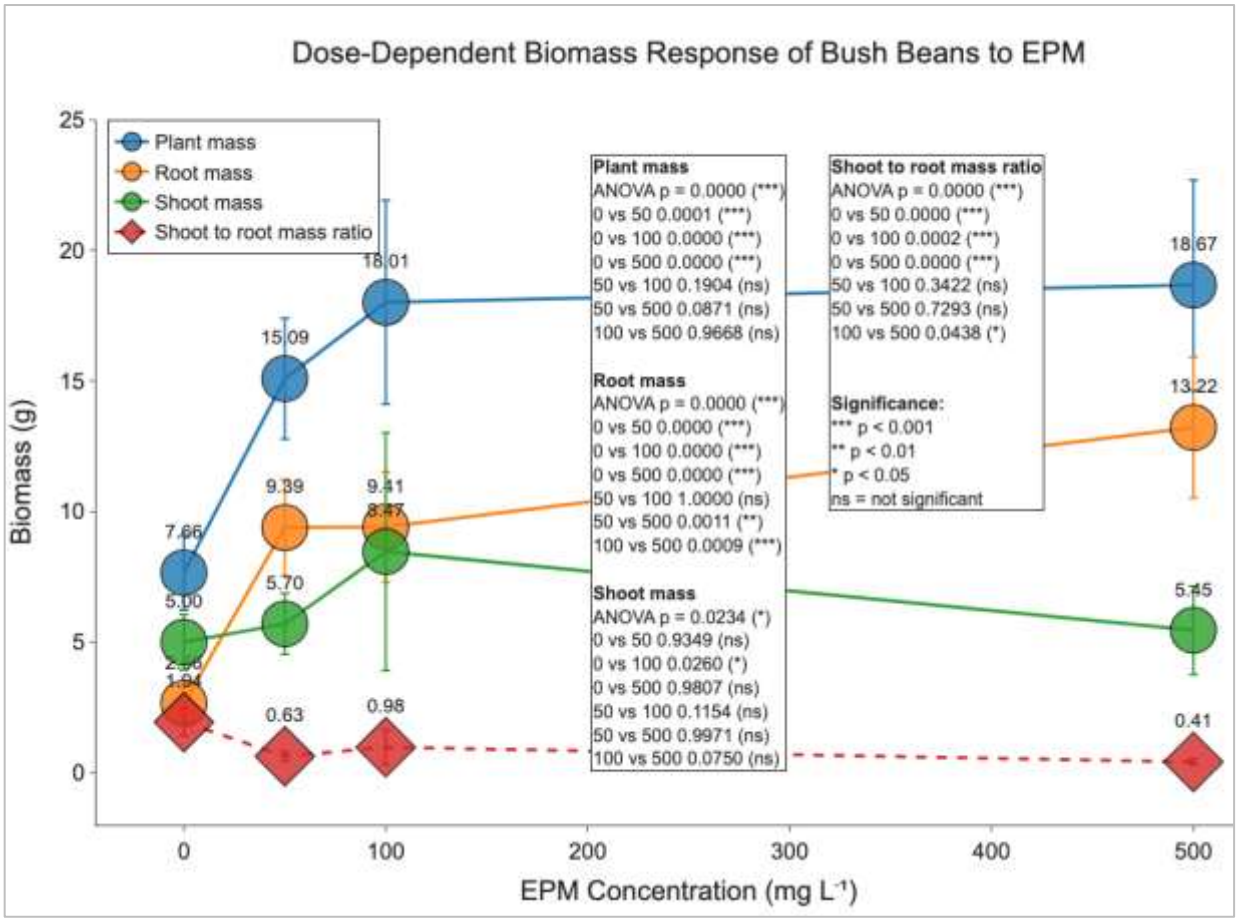


Figure 5 | Dose-dependent effects of EPM on bush bean biomass and allocation patterns.

Total plant biomass, root biomass, shoot biomass (g), and shoot-to-root ratio were quantified following exposure to increasing EPM concentrations (0-500 mg L⁻¹). One-way ANOVA revealed a significant treatment effect for total plant biomass, root biomass, and shoot-to-root ratio ($P < 0.001$), whereas shoot biomass was not significantly affected ($P > 0.05$). Tukey's honestly significant

difference (HSD) test indicated that total and root biomass were significantly greater at 50-500 mg L⁻¹ relative to the control, with the strongest root stimulation observed at 500 mg L⁻¹. The shoot-to-root ratio varied significantly among treatments, reflecting EPM-induced shifts in biomass allocation. Points represent means and error bars denote standard deviation. Significance was determined using one-way ANOVA followed by Tukey's HSD multiple-comparison test.

Root elemental composition was analyzed to evaluate how EPM-mediated soil modification influences nutrient uptake and allocation (**Supplementary Fig. S7**). Principal component analysis (PCA) revealed clear treatment-dependent separation, with PC1 and PC2 explaining 90.3% of the total variance (61.6% and 28.7%, respectively; **Figure 6**). Roots from the 100 mg L^{-1} treatment clustered closely with the control, indicating a comparable multielement composition, whereas the 50 and 500 mg L^{-1} treatments were distinctly separated, reflecting concentration-dependent shifts in nutrient accumulation patterns. Loading analysis (**Supplementary Fig. S8**) confirmed contributions from multiple macro- and micronutrients. Although both lower and higher EPM concentrations led to increased elemental accumulation in roots, this did not correspond to improved reproductive performance. In contrast, the 100 mg L^{-1} treatment maintained a more balanced elemental profile and was associated with enhanced pod development (**Figure 4c**).

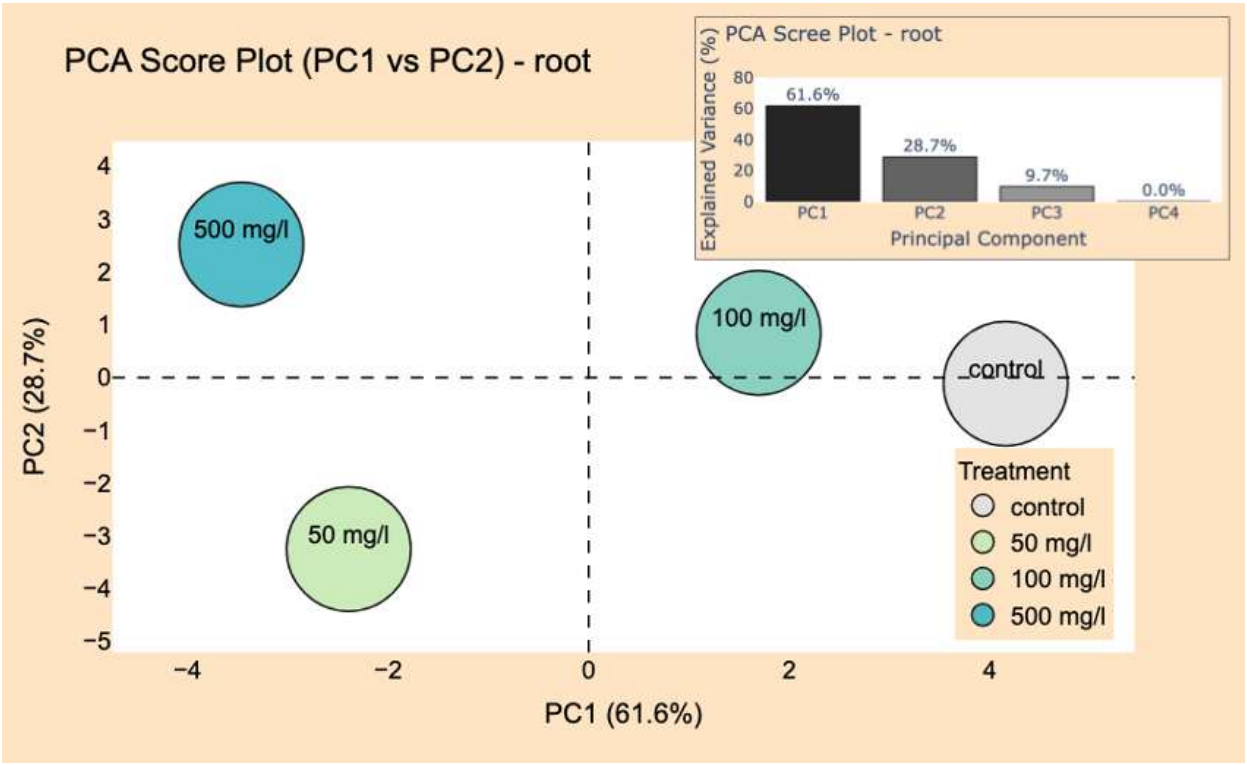


Figure 6 | Principal component analysis (PCA) score plot of elemental composition in bean roots grown under different EPM concentrations.

PC1 and PC2 together explain 90.3% of the total variance (PC1: 61.6%, PC2: 28.7%). Roots treated with 100 mg L^{-1} EPM cluster closely with control samples, indicating a similar elemental profile, whereas roots exposed to 50 mg L^{-1} and 500 mg L^{-1} EPM show clear separation from the control and from each other. The inset scree plot shows the percentage contribution of each principal component to the total variance.

Transcriptomic responses

To assess whether EPM-induced changes in soil structure translate into biological responses at the molecular level, root transcriptomes were analyzed following treatment with 125 mg L^{-1} EPM. Based on the observed increases in

biomass and lateral root development, we hypothesized that EPM-mediated modification of the soil environment alters gene expression pathways associated with root development and adaptive stress responses. *Arabidopsis thaliana* was used as a model system due to its well-characterized regulatory networks and suitability for transcriptomic analysis (JEFFREY CHEN et al. 2004). Representative root morphology is shown in **Supplementary Figure S9**.

Comparison of gene expression changes obtained by RNA sequencing and RT-qPCR showed strong agreement (R^2 = 0.80;

Figure 7), confirming the reliability of the dataset. EPM treatment induced coordinated upregulation of genes associated with stress adaptation and developmental regulation, including heat shock proteins (e.g., HSP22.0, HSP18.2, HSP17.6B) and regulatory genes such as SPL5 and TT4. Concurrent downregulation of a subset of genes was also observed, indicating broad transcriptional reprogramming in response to EPM treatment. Minor differences in fold-change magnitude between RNA-seq and qPCR were consistent with known methodological differences in sensitivity and dynamic range.

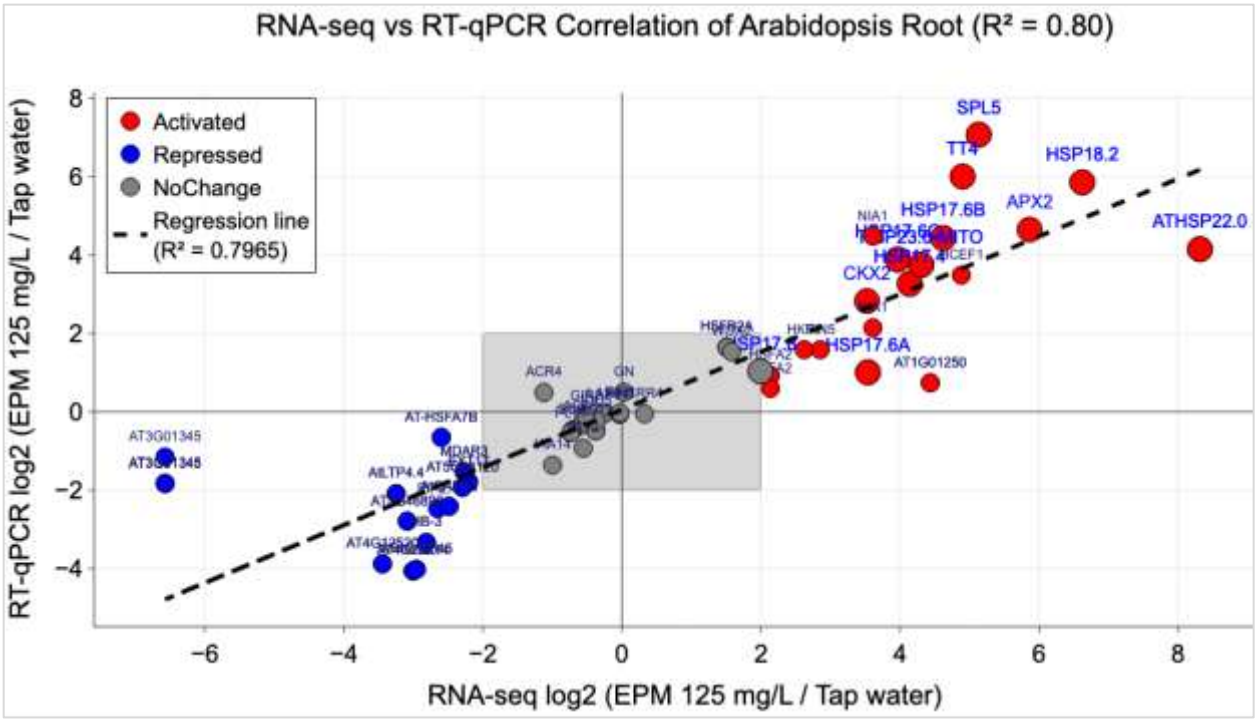


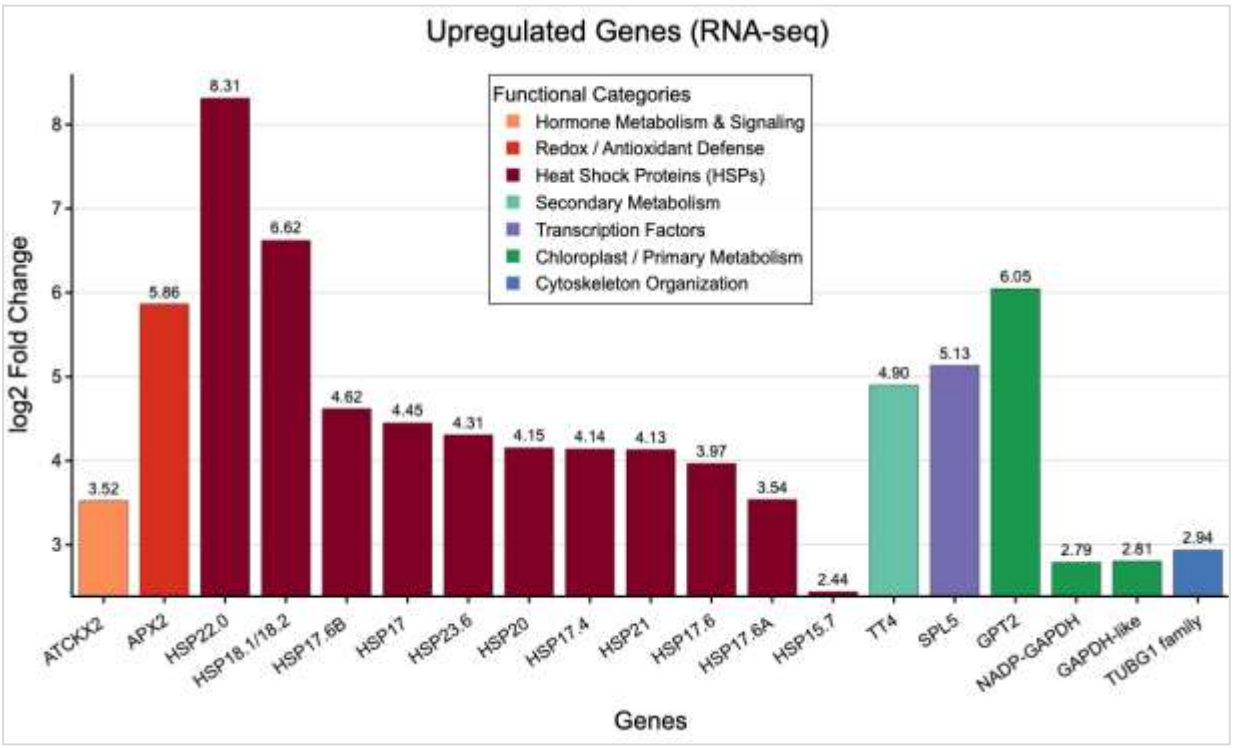
Figure 7 | Correlation between RNA-seq and RT-qPCR measurements of gene expression under 125 mg L^{-1} EPM treatment.

Scatter plot comparing log_2 fold-changes (125 mg L^{-1} EPM relative to tap water) obtained by RNA-seq (x-axis) and RT-qPCR (y-axis). Each point represents an individual gene. Red dots indicate significantly upregulated genes, blue dots indicate downregulated genes, and grey dots represent genes with no significant change. Selected genes discussed in detail in the main text including small heat shock proteins, CTX2, APX2, TT4, and SPL5 are shown with enlarged markers and royal blue text with larger font size for emphasis. The dashed line denotes the linear regression fit (R^2 = 0.7965). Strong concordance across a broad dynamic range confirms the reliability of RNA-seq quantification, with minor compression of extreme fold-changes observed in RT–qPCR measurements.

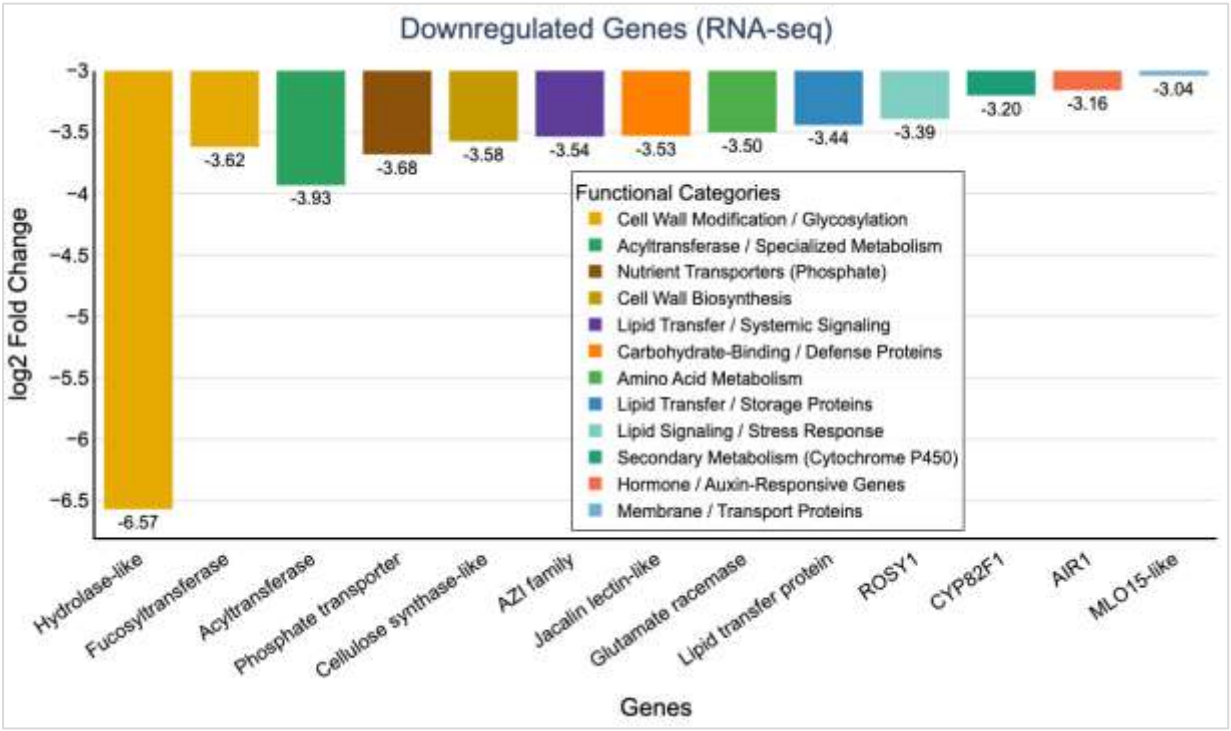
Following cross-platform validation of RNA-seq results using RT-qPCR (

Figure 7), differentially expressed genes were classified into up- and downregulated groups to clarify functional responses to EPM-mediated soil modification (**Figure 8**). Upregulated genes (**Figure 8a**) included those associated

with hormonal regulation, redox processes, stress adaptation, and developmental responses. Increased expression of ATCKX2, APX2, TT4, SPL5, GPT2, GAPDH isoforms, and multiple heat shock proteins (HSP22.0, HSP18.1/18.2, HSP15.7) was observed following EPM treatment. Genes associated with cytoskeletal organization, including TUBG1, were also induced. Detailed expression data, including moderately responsive genes, are provided in **Supplementary Fig. S10**. Downregulated genes (**Figure 8b**) included transcripts associated with cell wall modification, lipid transfer, nutrient acquisition, and stress-associated signaling pathways. Reduced expression was observed for glycosyltransferases, cellulose synthase-like genes, lipid transfer proteins, the phosphate transporter PHT1;3, phenylpropanoid-associated genes, and defense-related genes including AT5G35940 and AT2G44110. Downregulation of AT3G19550 was also detected, indicating alterations in amino acid metabolic pathways.



(a)



(b)

Figure 8 | Functional categorization of upregulated and downregulated genes in response to 125 mg L⁻¹ EPM (RNA-seq).

(a) Bar plot showing log₂ fold-change values for significantly upregulated genes grouped by functional categories. Heat shock proteins (HSPs) constitute the dominant class, exhibiting the highest induction levels, followed by genes involved in redox/antioxidant defense (e.g., APX2), chloroplast metabolism (e.g., GPT2, GAPDH isoforms), transcriptional regulation (SPL5), hormone metabolism (ATCKX2), secondary metabolism (TT4), and cytoskeletal organization (TUBG1 family). The data indicate extensive activation of proteostasis and redox pathways under EPM treatment.

(b) Bar plot showing log₂ fold-change values for significantly downregulated genes grouped by functional categories. Repressed genes include those associated with cell wall modification (cellulose synthase-like, fucosyltransferase), nutrient transport (PHT1;3), lipid transfer and signaling, amino acid and carbohydrate metabolism, and hormone-responsive pathways (AIR1). The coordinated repression of growth- and transport-related processes suggests a shift toward stress-adaptive transcriptional programming.

Temporal transcriptional responses

To evaluate whether EPM-induced transcriptional responses are transient or sustained, temporal expression patterns of two representative genes, TT4 and SPL5, were quantified using RT-qPCR (**Figure 9**). Plants were grown in soil and subsequently transferred to sand, with root tissues sampled at 3, 9, and 21 days. TT4 was selected as a marker associated with secondary metabolism, while SPL5 represents a regulatory gene involved in developmental signaling processes. TT4 exhibited a sustained increase in expression over time. Transcript levels increased approximately 10-fold at day 3, 22.5-fold at day 9, and reached 50.7-fold by day 21. In contrast, SPL5 displayed a transient expression profile. Transcript abundance was strongly suppressed at day 3 (~0.02-fold), followed by a marked increase at day 9 (~32.8-fold), and returned to near-baseline levels by day 21 (~1.07-fold).

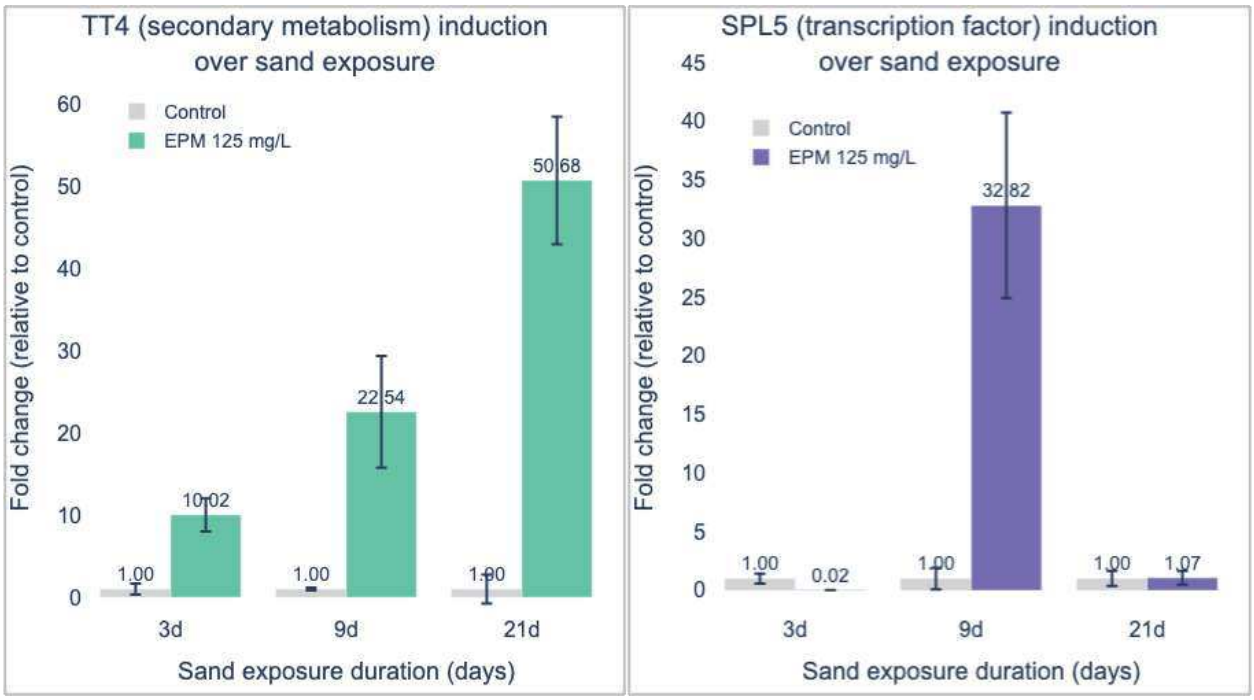


Figure 9 | Time-dependent induction of TT4 and SPL5 under EPM treatment.

Grouped bar plot on left side shows normalized TT4 expression in control and EPM-treated plants at 3, 9, and 21 days. TT4 exhibits strong early induction at day 9 (22.5-fold) and pronounced continuous amplification at day 21 (50.7-fold). Error bars represent standard deviation of biological replicates. Sustained activation indicates prolonged modulation of flavonoid biosynthesis under EPM exposure. Grouped bar plot on right side shows normalized SPL5 expression at 3, 9, and 21 days. SPL5 displays strong induction at day 9 (32.8-fold) and return to near-baseline levels by day 21. The data indicate that SPL5 functions as an early and transient transcriptional regulator in the EPM response.

Discussions

Pore-scale organization governs soil functional behavior

The contrasting structural responses induced by EPM and XG in **Figure 1** indicate fundamentally different modes of soil pore restructuring. The gradual and spatially uniform increase in strength observed for EPM suggests distributed interparticle interactions that stabilize soil structure without extensive disruption of pore continuity. This behavior is consistent with compliant polymer coatings at grain contacts that generate a connected load-transfer network while maintaining pore accessibility. In contrast, the greater variability and localized consolidation observed in XG-treated systems are consistent with gel-like pore filling and heterogeneous particle aggregation. Although this configuration produced higher bulk mechanical strength, the associated increase in tortuosity and pore heterogeneity likely reduced effective transport pathways within the rhizosphere. These findings demonstrate that soil functional behavior depends not only on the magnitude of mechanical reinforcement but also on the spatial organization and connectivity of pore networks. Preservation of pore accessibility is particularly important for water transport, gas diffusion, and root penetration, highlighting pore-permissive restructuring as a key mechanism linking soil physical architecture to plant establishment.

Root establishment

The contrasting plant responses observed between EPM- and XG-treated systems are consistent with their distinct pore-scale structural organizations. Previous studies have shown that XG can form heterogeneous, gel-like domains within granular media (Kumar et al. 2024), generating localized regions of reduced pore connectivity and increased mechanical impedance. Such structural heterogeneity may restrict root penetration, limit gas exchange, and reduce effective access to water and nutrients despite greater bulk soil strength. In contrast, EPM-treated soils maintained a more spatially uniform and connected pore network, providing pathways that support both structural stability and biological accessibility.

The strong Barmuda grass root response observed in EPM-amended systems in **Figure 2**, is consistent with the pore-scale structural characteristics identified in the physical analyses, where a connected and accessible pore network likely facilitates root penetration, water uptake, and nutrient acquisition. The proportional increase in shoot and root biomass in **Figure 3**, together with the stable shoot-to-root ratio, suggests that EPM-mediated soil restructuring supports integrated plant growth without inducing stress-related or compensatory allocation responses. In contrast, the absence of growth enhancement in XG-treated sand indicates that increased bulk soil strength alone is insufficient to improve plant performance when pore accessibility is constrained.

Dose-dependent performance

The concentration-dependent responses observed in EPM-amended bush beans in **Figure 4** and **Figure 5** indicate that plant performance is governed by an optimal balance between soil structural modification and rhizosphere accessibility. At low to intermediate concentrations, EPM likely maintains pore continuity that support efficient root-soil interactions, thereby promoting coordinated root development and reproductive performance. In contrast, the extensive root proliferation observed at the highest EPM concentration did not translate into enhanced shoot biomass and pod production.

The root elemental profile in **Figure 6** among EPM treatments indicate that nutrient availability alone does not determine plant productivity. At intermediate EPM concentrations, the enhanced development of more nutritious bean pods suggests that pore-permissive restructuring supports effective root-to-shoot and root-to-fruit transport pathways. Together, these findings demonstrate that EPM-mediated soil restructuring influences not only plant growth magnitude but also biomass allocation patterns, highlighting the importance of maintaining functional soil-plant nutrient coupling when designing biologically accessible and environmentally sustainable soil amendment strategies.

Molecular responses

The observed transcriptional responses in

Figure 7 and **Figure 8** suggest that EPM-mediated modification of soil pore architecture and associated microenvironmental conditions, including hydration and aeration, are perceived by plant roots and translated into coordinated molecular adjustments. Upregulated genes indicate activation of integrated hormonal, redox, and developmental processes associated with root system adaptation. Increased expression of ATCKX2 suggests modulation of cytokinin turnover, shifting hormonal balance toward conditions that favor lateral root initiation and spatial root expansion (Laplaze et al. 2007), (Bishopp et al. 2011). Concurrent upregulation of APX2 reflects enhanced

regulation of reactive oxygen species (ROS), which function as key signaling intermediates in root development under changing environmental conditions. Additional strong induction of heat shock proteins (HSP22.0, HSP18.1/18.2, HSP15.7) suggests enhanced cellular stabilization mechanisms during active growth in modified soil environments (Collier and Benesch 2020). Upregulation of TT4 further links secondary metabolism to root development through regulation of flavonoid-mediated auxin transport and ROS balance, supporting fine-scale control of lateral root formation (Peer and Murphy 2007), (Chapman and Muday 2021). Increased expression of SPL5, GPT2, and GAPDH isoforms reflects broader developmental and metabolic adjustments required to sustain growth under altered soil physical conditions (Gao et al. 2018), (Pastuglia et al. 2006). Changes in cytoskeletal-related gene expression (e.g., TUBG1) indicate structural reorganization associated with cell expansion and root system remodeling. Collectively, these transcriptional responses provide mechanistic evidence linking soil structural modification to enhanced root development and plant performance in EPM-amended systems.

In contrast, downregulated genes reveal a coordinated reduction in stress-associated, structural remodeling, and defense-related pathways. Repression of genes involved in cell wall modification (e.g., glycosyltransferases and cellulose synthase-like genes) suggests reduced need for structural reinforcement in a mechanically buffered and more stable soil environment (Pauly and Keegstra 2016). Downregulation of lipid transfer and stress-associated signaling genes indicates attenuation of cuticle- and dehydration-related responses, consistent with improved moisture conditions in EPM-treated substrates (Speicher et al. 2018), (Cameron et al. 2006). Nutrient acquisition pathways were also modulated, including reduced expression of the high-affinity phosphate transporter PHT1;3, suggesting altered nutrient demand or improved nutrient availability under EPM conditions (Nussaume et al. 2011), (Remy et al. 2012). Additionally, suppression of phenylpropanoid and defense-related genes indicates reduced allocation to stress-induced secondary metabolism (Chakraborty et al. 2023). Finally, repression of defense-associated genes, including AT5G35940 (Jacalin lectin-like) and AT2G44110 (MLO-like), points to reduced activation of biotic and abiotic stress pathways (Alagarasan 2024), (Miklis et al. 2007), while downregulation of AT3G19550 (glutamate racemase) suggests adjustments in amino acid metabolism and nitrogen allocation (Walker and van der Donk 2016).

The temporal expression profiles of TT4 and SPL5 in **Figure 9** suggest that EPM-mediated soil modification induces sequential phases of molecular adaptation. Sustained upregulation of TT4 indicates progressive activation of secondary metabolic pathways associated with flavonoid biosynthesis, which plays important roles in auxin transport, reactive oxygen species (ROS) regulation, and environmental adaptation (Mierziak et al. 2014). The continued increase in TT4 expression over time therefore suggests long-term metabolic adjustment rather than a transient stress response. In contrast, the transient behavior of SPL5 is consistent with an early regulatory response involved in initiating downstream developmental adaptation. The rapid suppression followed by temporary induction and eventual stabilization suggests dynamic transcriptional regulation during acclimation to altered soil physical conditions. Such temporal patterns are consistent with signaling networks that integrate environmental and hormonal cues to regulate root developmental plasticity (Barrera-Rojas et al. 2020). Together, these transcriptional shifts support a model in which EPM-mediated pore restructuring triggers a transition from stress-responsive metabolism toward a more stable and resource-efficient physiological state.

Proposed mechanism

When soil is dense, soil porosity decreases, which restricts the diffusion of oxygen and the volatile hormone ethylene. This restricted diffusion leads to an accumulation of ethylene in the root tissue (Kirschner 2024). This physical stress signal (ethylene) triggers downstream responses, including the expression of stress-induced CKX (Cytokinin Oxidase) genes, that permanently degrade the plant hormone cytokinin. Because cytokinin typically promotes cell division, its degradation serves as a protective mechanism that arrests root elongation, allowing the root to thicken so it can physically force its way through the dense soil layer (Werner et al. 2010).

The framework summarized in **Figure 10** suggests that EPM-mediated modification of soil pore architecture induces coordinated hormonal, redox, metabolic, and developmental responses that collectively regulate adaptive root system development. Central to this response is a shift in hormonal balance toward auxin-dominated signaling, likely associated with induction of ATCKX2, which promotes cytokinin degradation.

This hormonal rebalancing appears closely linked to redox regulation. Upregulation of APX2 suggests modulation of reactive oxygen species (ROS) homeostasis, maintaining signaling conditions that support cell proliferation and differentiation under altered soil physical environments. Concurrent induction of TT4 further indicates activation of flavonoid biosynthesis pathways known to regulate auxin transport and ROS distribution, contributing to integrated auxin–ROS control of root development. Induction of small heat shock proteins suggests enhanced cellular stabilization and protein protection during adaptation to modified rhizosphere conditions. Increased expression of SPL5, GPT2, GAPDH isoforms, and TUBG1 further indicates broader transcriptional, metabolic, and cytoskeletal reprogramming associated with sustained root growth and structural remodeling.

Together, these findings support a model in which EPM-induced soil pore restructuring modifies rhizosphere physical conditions and triggers coordinated molecular responses regulating hormonal signaling, redox balance, metabolism, and root developmental plasticity. This integrated response links soil physical architecture directly to plant functional adaptation and resilience in degraded soil environments.

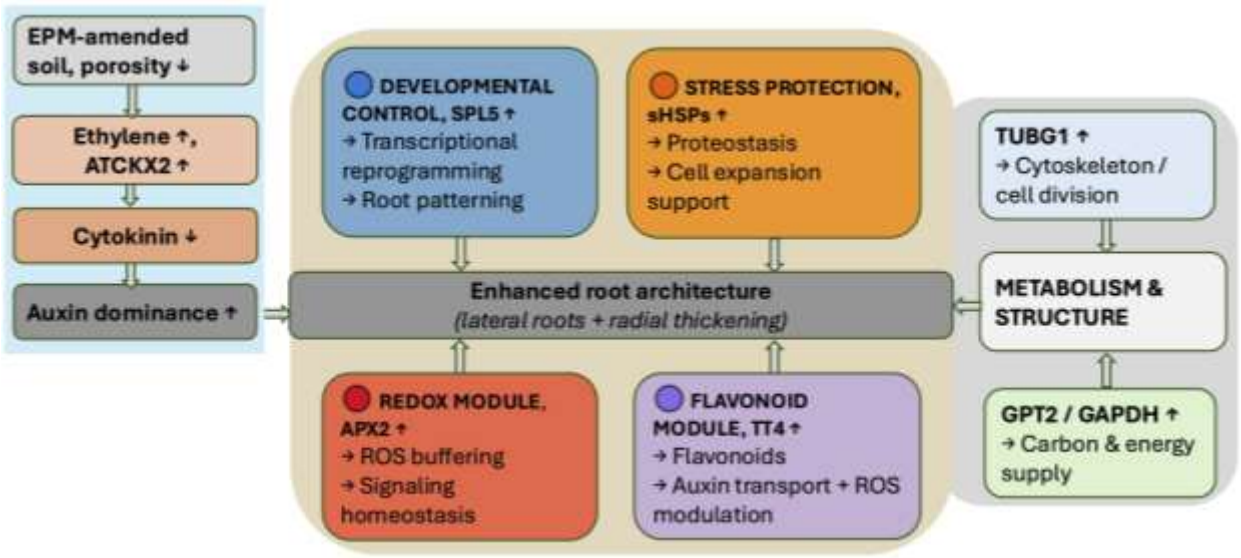


Figure 10 | Mechanism of EPM-induced regulatory network governing adaptive root development.

Schematic representation of the molecular pathways associated with root growth in EPM-amended soil. Densification of soil increases the ethylene in roots which induces ATCKX2. The induction of ATCKX2 promotes cytokinin degradation, shifting hormonal balance toward auxin-dominant signaling and facilitating lateral root initiation. This root architecture development is coordinated with redox regulation through APX2-mediated control of reactive oxygen species (ROS) and TT4-dependent flavonoid biosynthesis, which together modulate auxin transport and signaling. Concurrent upregulation of small heat shock proteins (sHSPs) supports proteostasis under dynamic substrate conditions, while SPL5 reflects broader transcriptional reprogramming of developmental pathways. Enhanced expression of metabolic (GPT2, GAPDH) and structural (TUBG1) genes indicates reallocation of carbon resources and cytoskeletal remodeling required for sustained root growth.

Conclusions

This study demonstrates that microbially derived biopolymers regulate soil-plant system behavior through coupled modifications of soil pore architecture and plant functional responses. Ethanol-precipitable material (EPM) and xanthan gum (XG) induce fundamentally different soil structural configurations. EPM generates a spatially uniform, pore-permissive network that preserves connectivity, whereas XG results in localized densification and increased pore heterogeneity, leading to reduced effective pore accessibility. These differences highlight that soil functional performance is governed not only by bulk mechanical strengthening but also by pore-scale organization and connectivity.

Plant responses closely reflected these contrasting soil environments, with EPM consistently promoting root proliferation and biomass accumulation in sandy soils, while XG showed limited plant growth enhancement despite greater mechanical reinforcement. In soil-based systems, EPM exhibited a concentration-dependent effect, with optimal plant performance at intermediate levels, indicating a balance between structural support and root accessibility. Elemental uptake patterns further suggest improved nutrient acquisition under pore configurations that maintain continuity and rhizosphere transport pathways.

At the system level, these results support a mechanistic framework in which pore-permissive soil restructuring regulates plant establishment through modulation of rhizosphere accessibility and root developmental responses. Overall, this work demonstrates that optimizing soil pore architecture for biological accessibility, rather than maximizing mechanical strength alone, is critical for enhancing plant-soil functional integration in degraded sandy soils.

Future work

Future research should further elucidate how microbially derived EPM-driven modifications of soil pore architecture translate into functional outcomes in coupled soil-plant-environment systems. A key priority is to establish quantitative linkages between μCT-derived pore-scale descriptors (e.g., connectivity, pore-throat size distribution, and tortuosity) and root system architecture, enabling predictive relationships between soil structural configuration and root developmental patterns.

In addition, direct characterization of soil hydraulic and gas transport properties, including water retention behavior, unsaturated hydraulic conductivity, and oxygen diffusivity, is essential to determine how pore-permissive structural modifications regulate rhizosphere water and aeration dynamics under realistic environmental conditions. The observed concentration-dependent effects of EPM on plant performance also warrant further mechanistic

investigation, particularly regarding how application rate influences carbon allocation, hormonal regulation, and developmental transitions, including reproductive output.

Long-term studies are needed to assess the stability of EPM-induced soil pore structures under dynamic environmental cycles such as wetting-drying and mechanical disturbance, and to evaluate the persistence of associated plant growth responses. Furthermore, the transferability of these effects across contrasting soil textures, climatic conditions, and plant species should be systematically assessed to define the boundaries of applicability.

Finally, rhizosphere-scale investigations are required to determine whether EPM-induced structural modifications also influence microbial community assembly and plant-microbe interactions, thereby linking soil physical architecture with biological and ecosystem-level functioning.

Acknowledgement

We gratefully acknowledge financial support from the U.S. Army Corps of Engineers, Engineer Research and Development Center (ERDC), under Grant No. W912HZ2120034 and Subcontract No. 45085319245.

Results in this report are derived from research conducted through the eBERlight program (7-BM), funded by the U.S. Department of Energy (DOE) Office of Biological and Environmental Research (BER) and supported by the Advanced Photon Source (APS), (DOIs: link), a DOE, Office of Science, user facility operated by Argonne National Laboratory under Contract No. DE-AC02-06CH11357. We thank Alex Lavens and Dr. Alan Kastengren for supporting the experiment.

We also acknowledge support from the Government of Israel, Ministry of Defense, under Contract No. 4441418256.

Computational processing of the micro-CT data was performed using SeaWulf, the high-performance computing cluster at Stony Brook University.

References

Alagarasan G (2024) Duality of jacalin-related lectin: Master regulator and chaperone. Plant Commun 5:100825. https://doi.org/10.1016/j.xplc.2024.100825

Barrera-Rojas CH, Rocha GHB, Polverari L, et al (2020) miR156-targeted SPL10 controls Arabidopsis root meristem activity and root-derived de novo shoot regeneration via cytokinin responses. J Exp Bot 71:934–950. https://doi.org/10.1093/jxb/erz475

Bengough AG, Bransby MF, Hans J, et al (2006) Root responses to soil physical conditions; growth dynamics from field to cell. J Exp Bot 57:437–447. https://doi.org/10.1093/jxb/erj003

Bishopp A, Help H, El-Showk S, et al (2011) A mutually inhibitory interaction between auxin and cytokinin specifies vascular pattern in roots. Curr Biol CB 21:917–926. https://doi.org/10.1016/j.cub.2011.04.017

Cameron KD, Teece MA, Smart LB (2006) Increased Accumulation of Cuticular Wax and Expression of Lipid Transfer Protein in Response to Periodic Drying Events in Leaves of Tree Tobacco. Plant Physiol 140:176–183. https://doi.org/10.1104/pp.105.069724

Chakraborty P, Biswas A, Dey S, et al (2023) Cytochrome P450 Gene Families: Role in Plant Secondary Metabolites Production and Plant Defense. J Xenobiotics 13:402–423. https://doi.org/10.3390/jox13030026

493 Chapman JM, Muday GK (2021) Flavonols modulate lateral root emergence by scavenging reactive oxygen species
494 in *Arabidopsis thaliana*. J Biol Chem 296:100222. https://doi.org/10.1074/jbc.RA120.014543

495 Cheng Z, Geng X (2023) Investigation of unconfined compressive strength for biopolymer treated clay. Constr Build
496 Mater 385:131458. https://doi.org/10.1016/j.conbuildmat.2023.131458

497 Collier MP, Benesch JLP (2020) Small heat-shock proteins and their role in mechanical stress. Cell Stress Chaperones
498 25:601–613. https://doi.org/10.1007/s12192-020-01095-z

499 Feng M, Zhang M, Cai P, et al (2026) Increased microbial extracellular polymeric substances as a key factor in deep
500 soil organic carbon accumulation. Soil Biol Biochem 212:109998.
501 https://doi.org/10.1016/j.soilbio.2025.109998

502 Gao R, Wang Y, Gruber MY, Hannoufa A (2018) miR156/SPL10 Modulates Lateral Root Development, Branching
503 and Leaf Morphology in Arabidopsis by Silencing AGAMOUS-LIKE 79. Front Plant Sci 8:2226.
504 https://doi.org/10.3389/fpls.2017.02226

505 JEFFREY CHEN Z, WANG J, TIAN L, et al (2004) The development of an Arabidopsis model system for genome-
506 wide analysis of polyploidy effects. Biol J Linn Soc Linn Soc Lond 82:689–700.
507 https://doi.org/10.1111/j.1095-8312.2004.00351.x

508 Kirschner GK (2024) A compact topic: How ethylene controls crown root development in compacted soil. Plant Cell
509 36:2063–2064. https://doi.org/10.1093/plcell/koae091

510 Kolb E, Legué V, Bogeat-Triboulot M-B (2017) Physical root–soil interactions. Phys Biol 14:065004.
511 https://doi.org/10.1088/1478-3975/aa90dd

512 Kumar S, Yadav BD, Raj R (2024) A review on the application of biopolymers (xanthan, agar and guar) for sustainable
513 improvement of soil. Discov Appl Sci 6:393. https://doi.org/10.1007/s42452-024-06087-7

514 Lal R (2001) Soil degradation by erosion. Land Degrad Dev 12:519–539. https://doi.org/10.1002/ldr.472

515 Laplaze L, Benkova E, Casimiro I, et al (2007) Cytokinins act directly on lateral root founder cells to inhibit root
516 initiation. Plant Cell 19:3889–3900. https://doi.org/10.1105/tpc.107.055863

517 Larson S, Ballard J, Griggs C, et al (2012) An Innovative Non-Petroleum Rhizobium Tropici Biopolymer Salt for Soil
518 Stabilization. American Society of Mechanical Engineers Digital Collection, pp 1279–1284

519 Mierziak J, Kostyn K, Kulma A (2014) Flavonoids as Important Molecules of Plant Interactions with the Environment.
520 Molecules 19:16240–16265. https://doi.org/10.3390/molecules191016240

521 Miklis M, Consonni C, Bhat RA, et al (2007) Barley MLO Modulates Actin-Dependent and Actin-Independent
522 Antifungal Defense Pathways at the Cell Periphery. Plant Physiol 144:1132–1143.
523 https://doi.org/10.1104/pp.107.098897

524 Nestler C, Larson S, Nijak G, et al (2016) Evaluation of Rhizobium tropici-derived Biopolymer for Erosion Control
525 of Protective Berms. Field Study

526 Nikitin V (2023) TomocuPy – efficient GPU-based tomographic reconstruction with asynchronous data processing. J
527 Synchrotron Radiat 30:179–191. https://doi.org/10.1107/S1600577522010311

528 Nussaume L, Kanno S, Javot H, et al (2011) Phosphate Import in Plants: Focus on the PHT1 Transporters. Front Plant
529 Sci 2:83. https://doi.org/10.3389/fpls.2011.00083

Osman KT (2018) Sandy Soils. In: Osman KT (ed) Management of Soil Problems. Springer International Publishing, Cham, pp 37–65

Palhares Farias T, de Melo Castro E, Marucci Pereira Tangerina M, et al (2022) Rhizobia exopolysaccharides: promising biopolymers for use in the formulation of plant inoculants. Braz J Microbiol 53:1843–1856. https://doi.org/10.1007/s42770-022-00824-z

Pastuglia M, Azimzadeh J, Goussot M, et al (2006) Gamma-tubulin is essential for microtubule organization and development in Arabidopsis. Plant Cell 18:1412–1425. https://doi.org/10.1105/tpc.105.039644

Pauly M, Keegstra K (2016) Biosynthesis of the Plant Cell Wall Matrix Polysaccharide Xyloglucan*. Annu Rev Plant Biol 67:235–259. https://doi.org/10.1146/annurev-arplant-043015-112222

Peer WA, Murphy AS (2007) Flavonoids and auxin transport: modulators or regulators? Trends Plant Sci 12:556–563. https://doi.org/10.1016/j.tplants.2007.10.003

Raj N, Selvakumar S, Soundara B, Kulanthaivel P (2023) Sustainable utilization of biopolymers as green adhesive in soil improvement: a review. Environ Sci Pollut Res 30:118117–118132. https://doi.org/10.1007/s11356-023-30642-1

Remy E, Cabrito TR, Batista RA, et al (2012) The Pht1;9 and Pht1;8 transporters mediate inorganic phosphate acquisition by the Arabidopsis thaliana root during phosphorus starvation. New Phytol 195:356–371. https://doi.org/10.1111/j.1469-8137.2012.04167.x

Sloutski A, Chen C, Gao J, et al (2025) Rhizobium tropici biopolymer enhances lateral root formation in agar-grown Arabidopsis. Biochem Biophys Res Commun 775:152125. https://doi.org/10.1016/j.bbrc.2025.152125

Soldo A, Miletić M, Auad ML (2020) Biopolymers as a sustainable solution for the enhancement of soil mechanical properties. Sci Rep 10:267. https://doi.org/10.1038/s41598-019-57135-x

Speicher TL, Li PZ, Wallace IS (2018) Phosphoregulation of the Plant Cellulose Synthase Complex and Cellulose Synthase-Like Proteins. Plants 7:52. https://doi.org/10.3390/plants7030052

Walker MC, van der Donk WA (2016) The Many Roles of Glutamate in Metabolism. J Ind Microbiol Biotechnol 43:419–430. https://doi.org/10.1007/s10295-015-1665-y

Werner T, Nehnevajova E, Köllmer I, et al (2010) Root-Specific Reduction of Cytokinin Causes Enhanced Root Growth, Drought Tolerance, and Leaf Mineral Enrichment in Arabidopsis and Tobacco[C][W][OA]. Plant Cell 22:3905–3920. https://doi.org/10.1105/tpc.109.072694

Yiwei Fang, Rick Qian, Steven Yang, et al (2025) Biopolymer produced by Rhizobium Tropici: Chemistry, Water Retention, and Interactions with Clays. ISSMGE. https://doi.org/10.53243/ICBBG2025-125

Statements and Declarations

Funding

This work was supported by the U.S. Army Corps of Engineers, Engineer Research and Development Center (ERDC) under Grant No. W912HZ2120034 and Subcontract No. 45085319245.

Competing Interests

The authors have no relevant financial or non-financial interests to disclose.

Declaration of AI-assisted technologies

During the preparation of this manuscript, the authors used open-source tools to improve the clarity, readability, and language of the text. All content generated with the assistance of this tool was carefully reviewed and edited by the authors, who take full responsibility for the final published version of the manuscript. These tools were not used for data analysis, interpretation, or drawing scientific conclusions as part of the research process.

Author Contributions

All authors contributed to the study conception and design. Material preparation, data collection and analysis were performed by Kaniz Fatema, Aaron Sloutski, Jay G. Gao, Marcia Simon, Vitaly Citovsky, and Miriam Rafailovich. The first draft of the manuscript was written by Kaniz Fatema and Aaron Sloutski, and all authors commented on previous versions of the manuscript. All authors read and approved the final manuscript.

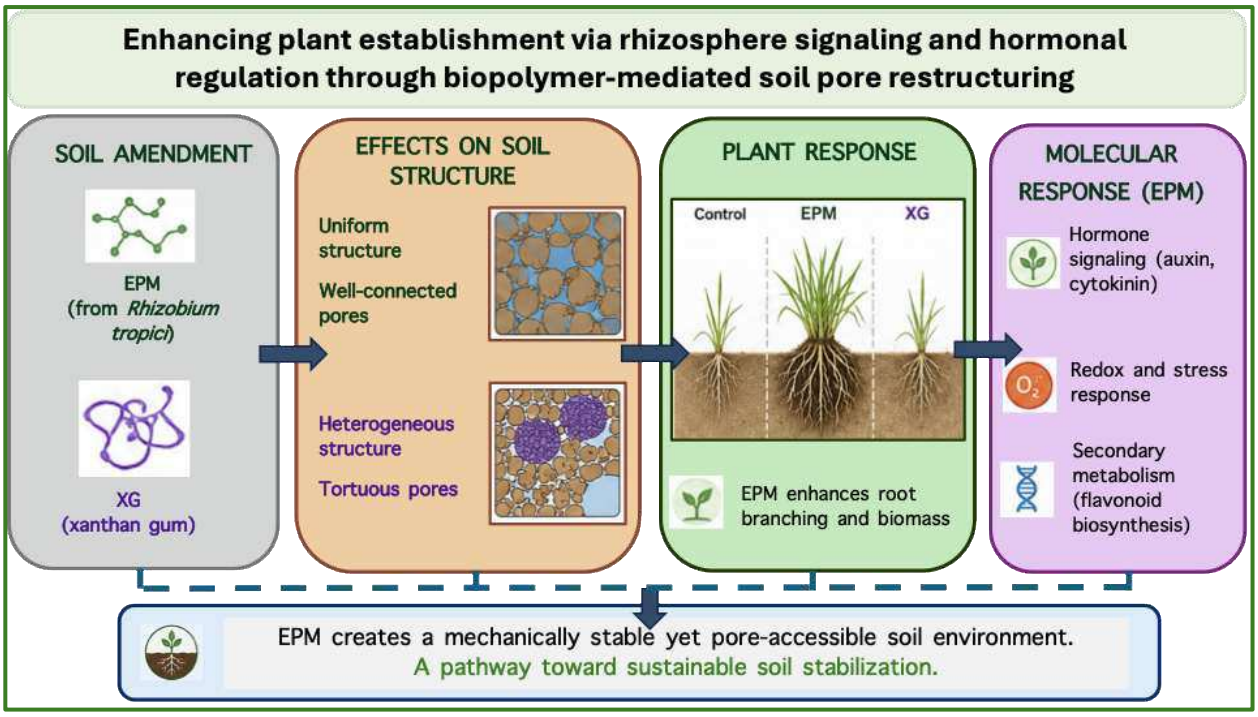
Data Availability

The datasets generated during and/or analyzed during the current study are available from the corresponding author on reasonable request. The relevant excel files and the Python codes for data analysis are uploaded on Zenodo (DOI: link) and GitHub.

Highlights

- Microbially derived ethanol-precipitable material (EPM) restructures sandy soil pore architecture while preserving pore connectivity and rhizosphere accessibility.
- EPM promotes root proliferation and increases plant biomass by more than fourfold, whereas xanthan gum induces pore heterogeneity and provides limited growth benefits.
- Plant responses exhibit a dose-dependent relationship with EPM, identifying an optimal balance between soil structural modification and rhizosphere function.
- Transcriptomic and RT-qPCR analyses reveal coordinated regulation of cytokinin turnover, auxin-associated signaling, flavonoid biosynthesis, and redox pathways linked to root development.
- Pore-permissive soil restructuring drives phenotypic and molecular adaptation, linking soil physical architecture to root system development and plant establishment.

Graphical abstract



Supplementary Files

This is a list of supplementary files associated with this preprint. Click to download.

- supplementaryfile.docx